Giant elastocaloric effect in ferroelectric $Ba_{0.5}Sr_{0.5}TiO_3$ alloys from first-principles

S. Lisenkov[*] and I. Ponomareva

Department of Physics, University of South Florida, Tampa, Florida 33620, USA

As the need for efficient energy converting devices has been rapidly increasing, the materials that exhibit large or even giant caloric responses have emerged as promising candidates for solid-state refrigeration, which is an energy-efficient and environmentally friendly alternative to the conventional refrigeration technology. However, despite recent ground breaking discoveries of giant caloric responses in some materials, they appear to remain one of nature's rarities. Here we predict the existence of giant elastocaloric effect in ferroelectric $Ba_{0.5}Sr_{0.5}TiO_3$ alloys, which adds one more member to this exclusive collection. Moreover, this computational finding reveals the multicaloric nature of such alloys, which could lead to new paradigms for cooling devices.

Caloric effects are associated with a reversible change in the temperature under adiabatic application of external fields.[1–12] Alternatively, they can be described as an isothermal change in entropy achieved by the application of the fields. A number of caloric effects can be deduced from inspection of thermodynamical relations with the most famous being magnetocaloric, electrocaloric, elastocaloric, and barocaloric effects. The caloric effects are particularly attractive for solid state refrigeration which is considered to be an energy efficient and environmentally friendly alternative to the current technology based on the vapor compression of hazardous gases.[13] Interestingly, while a wide variety of materials can exhibit caloric effects, these effects are minuscule for most of them.

Among the different caloric effects, the magnetocaloric effect in which the application of the magnetic field leads to a change in temperature is by far the most studied one. One of the reasons for that is that some magnetic materials were found to exhibit a giant magnetocaloric effect.[1,3,4] For example, a giant magnetocaloric effect in excess of 10 K was reported in $Gd_5(Si_2Ge_2)$ alloy.[1] It is believed that the ability of a material to exhibit a giant magnetocaloric effect is correlated with the existence of large magnetostructural transitions in the same material. In a giant magnetocaloric material the magnetic field induces a simultaneous change in magnetic as well as lattice entropies.[4] On the other hand, the ability of a material to undergo a large structural transition can give rise to another type of caloric effect—elastocaloric and barocaloric effects. In the elastocaloric (barocaloric) effect the adiabatic application of mechanical stress (pressure) leads to a change in the temperature. Recently a giant elastocaloric effect was found in shape-memory alloys.[7] Giant barocaloric effect was reported for the magnetic shape-memory alloys.[5] In fact, it was shown that the magnitude of such barocaloric effect can be comparable to the giant magnetocaloric effect in such materials. Moreover, the giant inverse barocaloric effect was discovered in magnetocaloric La-Fe-Si-Co compound.[6] It was proposed that such an effect may even exceed the giant magnetocaloric effect in the same compound.

The electric analogy of magnetocaloric effect is the electrocaloric effect where the adiabatic application of an electric field to a dielectric material results in a reversible change in the temperature. Similar to magnetocaloric effect, which derives its origin in the coupling of magnetic dipoles with magnetic field, the electrocaloric effect derives its origin from the coupling of electric dipoles with electric field. Interestingly, the analogy between the magnetocaloric and electrocaloric effects seems to suggest that the materials that exhibit strong coupling between structural distortions and electric dipoles may exhibit giant electrocaloric effect. One example of such materials is ferroelectrics. Indeed, for most ferroelectric phase transitions the onset of a ferroelectric phase is associated with fairly large structural distortions which gives rise to first-order character of such transitions.[14] Recently the giant electrocaloric effect was indeed found in ferroelectric alloys and polymers,[8,9,15,16] further expanding the family of giant caloric materials. However, one question still remains: does there exist an "electric" analogy of giant elastocaloric or barocaloric effect similar to the one found in giant magnetocaloric materials?[5,6] Such a giant effect(s) could be the "lost" member for the family of giant caloric responses and a new path to multicaloric materials.

In this paper we report the prediction of a giant electrically-mediated elastocaloric effect in ferroelectric alloys. This computational finding reveals that, in ferroelectrics, the two giant effects—electrocaloric and elastocaloric—may coexist and even couple, thus demonstrating the multicaloric nature of these materials. The intrinsic multicaloric materials in which one or more large caloric effects coexist are very rare. To the best of our knowledge, the only other example known to date is the giant magnetocaloric shape-memory alloys.[5,6] The finding of the "electric" counterpart of this intrinsic multicaloric material may become a critical step towards achieving solid-state cooling.[13]

Here we investigate the elastocaloric effect in ferroelectric alloy made of $Ba_{0.5}Sr_{0.5}TiO_3$ solid solution. Among the different ferroelectric alloys, the $Ba_xSr_{1−x}TiO_3$ family shows an unmatched tunability associated with the varying of alloy composition x. In fact, the Curie temperature depends strongly on the concentration x and ranges from 0 K in $SrTiO_3$ to up to 405 K in $BaTiO_3$. Such tunability is very attractive for caloric applications since most of the caloric effects are maximized in the vicinity of the Curie point. Being in the middle of the compositional range, $Ba_{0.5}Sr_{0.5}TiO_3$ is a good representative for the whole family of $Ba_xSr_{1−x}TiO_3$ alloys. Moreover, a giant electrocaloric effect was previously reported for this particular alloy.[16,17] $Ba_{0.5}Sr_{0.5}TiO_3$ undergoes three ferroelectric transitions: paraelectric cubic to ferroelectric tetragonal at

$T_C = 250$ K, ferroelectric tetragonal to ferroelectric orthorhombic at $T = 180$ K, and ferroelectric orthorhombic to ferroelectric rhombohedral at $T = 140$ K.[18]

The $Ba_{0.5}Sr_{0.5}TiO_3$ sample was modeled by a $16 \times 16 \times 16$ simulation supercell (20 480 particles) periodic along three Cartesian directions and with Ba, Sr atoms distributed randomly among the individual unit cells. The x, y, and z axis were chosen along [100], [010], and [001] crystallographic directions, respectively. The potential energy of the sample U^{pot} is given by the first-principles-based effective Hamiltonian of Ref. [19] which is defined in terms of the following degrees of freedom: local mode vectors (proportional to the local dipole moments in the sample's unit cells); inhomogeneous and homogeneous strain variables (that describe the local deformations of the unit cells). The Hamiltonian includes (i) the local mode self-energy, i.e., the energy of isolated local mode relative to that of a perfect cubic structure which contains both harmonic and unharmonic terms; (ii) short-range; (iii) long-range (dipole-dipole) interaction energy between the local modes belonging to different unit cells; (iv) the elastic energy (harmonic in strain); and (v) the energy associated with the on-site coupling between the local mode and local distortion (responsible for electrostriction). The latter energy is linear in strain and quadratic in local mode. This Hamiltonian reproduces accurately the experimental composition-temperature phase diagram of disordered $Ba_xSr_{1-x}TiO_3$ solid solution[19] and dynamical properties of $BaTiO_3$,[20] provides accurate predictions for $BaTiO_3/SrTiO_3$ superlattices,[21] and has been used recently to study a variety of properties of $Ba_xSr_{1-x}TiO_3$ alloys.[17,22,23]

To model the elastocaloric response we use our direct approach similar to the one reported in Ref. [16] for electrocaloric effect. This approach computes adiabatic temperature evolution under external field directly and without having to resort to the use of Maxwell equations. Technically, the computations are achieved by simulating isoenthalpic ensemble $H = const$. According to the enthalpic form of the first law of thermodynamics: $d\mathcal{H} = dQ - \varepsilon_i d\sigma_i - D_i dE_i$, where $\mathcal{H} = U - \sigma_i \varepsilon_i - E_i D_i$ is the enthalpy density. Here dQ is an infinitesimal quantity of heat received by a unit volume, and ε_i and σ_i are the components of the strain and stress tensors, respectively, written in Voigt notation. D_i and E_i are the ith Cartesian component of the electric displacement field and the electric field, respectively, and U is the internal energy density. Since the elastocaloric effect of interest is an adiabatic process ($dQ = 0$) that occurs under slowly varying stress fields ($\sigma_i \approx const$) and zero electric field, it can be considered as an isoenthalpic process $\mathcal{H} = const$. To simulate the isoenthalpic ensemble we follow the spirit of microcanonical Monte Carlo simulations[24] and introduce extra degrees of freedom, called "demons" (analogous to the conjugate momenta in the microcanonical formulations), that absorb/carry/redistribute energy to achieve $\mathcal{H} = const$ simulations. In our simulations the enthalpy of the supercell is $\mathcal{H} = (U^{pot} + \sum_{j=1}^{n^{dem}} E_j^{dem} - V\sigma_i\varepsilon_i) = H + \sum_{j=1}^{n^{dem}} E_j^{dem}$, where U^{pot} is the potential energy of the supercell given by the effective Hamiltonian, E_j^{dem} is the energy carried by the jth demon, while n^{dem} is the total number of demons in the supercell. V is the supercell volume. H is the enthalpy less the energy of all demons.
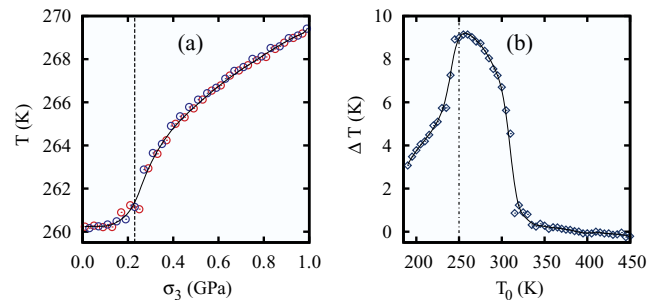

FIG. 1. (Color online) (a) The dependence of the sample temperature on the applied stress. Red and blue circles indicate data from heating and cooling simulations, respectively. The solid line is for use as a guide to the eye. Vertical dashed line indicates the point of stress-induced ferroelectric structural phase transition. (b) The dependence of the elastocaloric change in temperature on the initial temperature of the sample when the stress was slowly increased from 0 to 1 GPa. Dash-dotted line indicates the Curie point of the material in the absence of applied fields.

We include $n_j^{dem} = \text{integer}[(C_P - \frac{1}{V}\frac{\partial U^{pot}}{\partial T})/k_B] = 8$ demons per unit cell to correctly reproduce the computational heat capacity $C_P = 2.58$ MJ/K m^3. At each isoenthalpic Monte Carlo step, an update for a degree of freedom is attempted and compared with the energy of a randomly or sequentially picked demon E_j^{dem}. If $E_j^{dem} - \Delta H > 0$ the move is accepted and $H \rightarrow H + \Delta H$ and $E_j^{dem} \rightarrow E_j^{dem} - \Delta H$. One Monte Carlo sweep attempts to update all the degrees of freedom sequentially. The temperature is calculated after each sweep as $T = \sum_{j=1}^{n^{dem}} E_j^{dem}/k_B n^{dem}$ and is typically averaged over 20 000 sweeps.

In our direct approach we first equilibrate the sample at the desired temperature T_0 using 3×10^5 Monte Carlo sweeps of Metropolis algorithm.[25] We next switch to $\mathcal{H} = const$ simulations and apply normal tensile stress σ_3 acting on the plane perpendicular to the z axis. Specifically, σ_3 is slowly increased from 0 to 1 GPa at a rate of 1 kPa per one Monte Carlo sweep. Note that such stress range is comparable to the experimental stresses.[5,7] The temperature T at a given stress field σ_3 is calculated from the average demon energy obtained at the same stress.

Figure 1(a) shows the dependence of the temperature on the applied stress from both elastocaloric heating and cooling simulations. The initial temperature in the heating simulations is $T_0 = 260$ K which is 10 K above the Curie point. As the tensile stress increases the temperature increases as well thus establishing the existence of an elastocaloric effect in this material. Furthermore, we obtained very similar temperatures from both heating and cooling simulations which indicates that such processes are completely reversible and exhibit no or very little hysteresis. The most striking feature of the data, though, is the existence of giant elastocaloric effect in such material. Indeed the overall temperature change ΔT upon stress application is 9 K, which is in the range of temperature changes for other giant caloric effects.[1,3–9,16] Moreover, such ΔT is nearly identical to the electrocaloric temperature change in the same alloy under application of 600 kV/cm electric field.[16] Therefore, two giant caloric effects can coexist in
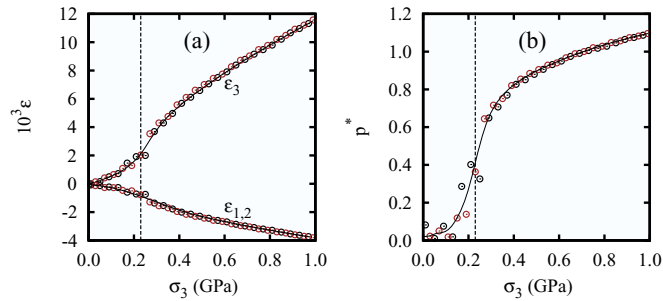
FIG. 2. (Color online) The dependence of the relative strains (a) and the ferroelectric order parameter (b) on the applied stress. Brown and black circles indicate data from heating and cooling simulations, respectively. The solid lines should be considered as guides to the eye. Vertical dashed lines indicate the point of stress-induced ferroelectric structural phase transition.

some ferroelectrics which reveals the multicaloric nature of these materials. Such intrinsic multicaloric ferroics are of particular value for emerging (near) room temperature cooling devices.[13]

Interestingly the $T(\sigma_3)$ curve in Fig. 1(a) is nonlinear. For the stresses below 0.2 GPa the temperature remains almost constant indicating that the elastocaloric effect is nearly negligible in this stress range. In the region 0.2–0.3 GPa the temperature increases sharply so that almost half of its total ΔT concentrates in this narrow region of stresses. As the stress further increases the temperature continues to rise, while beginning to show a saturation trend. We conducted simulations for other temperatures T_0 from tetragonal and paraelectric regions of $Ba_{0.5}Sr_{0.5}TiO_3$. The elastocaloric temperature change ΔT as a function of T_0 is presented in Fig. 1(b). Our data indicate that the giant elastocaloric effect exists in a wide range of temperatures near the Curie point of $Ba_{0.5}Sr_{0.5}TiO_3$ and peaks right at the Curie temperature T_C. In fact, ΔT in excess of 4 K was found for the temperatures 50 K below and above the Curie point, suggesting an extremely wide window of operational temperatures. In addition, given the strong dependence of $Ba_xSr_{1-x}TiO_3$ Curie temperatures on the alloy composition, it might be possible to stabilize large caloric responses in an even wider temperature range by heterostructuring $Ba_xSr_{1-x}TiO_3$ alloys.

To understand the origin of the giant elastocaloric effect in ferroelectric alloys we will focus on the changes in the material that occur under application of the stress. Figure 2(a) shows the dependence of the normal strain components $\varepsilon_i = \frac{a_i-a_0}{a_0}$ on the tensile stress σ_3. Here a_i is the lattice constant along the ith Cartesian direction, while a_0 is the equilibrium lattice constant of cubic $Ba_{0.5}Sr_{0.5}TiO_3$ at $T = 260$ K. It can be seen that ε_3 ($\varepsilon_{1,2}$) increases (decreases) smoothly with the applied stress and exhibits an inflection point at $\sigma_3^{tr} = 0.23$ GPa. This seems to point to a second-order-like stress-induced structural phase transition at σ_3^{tr}. Interestingly, second order phase transitions are usually associated with small or moderate caloric effects. Moreover, the change in the strain due to the stress is relatively small as compared to the strains developed in materials with giant elastocaloric effect.[7] These findings seem to suggest

that the structural transition itself cannot fully account for the observed giant elastocaloric effect.

To gain further insight we will look into the evolution of ferroelectric order parameter under the application of stress. Here we define the ferroelectric order parameter as the average dipole moment of the sample $p = \sum_j d_j/N$ projected onto the zth Cartesian direction. Here d_j is the zth component of the dipole moment of the particle j, and N is the total number of the dipoles. For convenience, we will use a reduced value for the order parameter defined as $p^* = p/p_0$, where p_0 is the average order parameter associated with the ferroelectric tetragonal phase of $Ba_{0.5}Sr_{0.5}TiO_3$. Note that we only report the ferroelectric order parameter along the direction conjugate to the direction of the applied stress. The order parameters along other directions are not affected by the applied stress and remain equal to zero. Figure 2(b) shows the evolution of the ferroelectric order parameter p^* under applied stress. The $p^*(\sigma_3)$ curve reveals that the material undergoes a stress-induced first-order-like ferroelectric phase transition that is associated with the condensation of ferroelectric order parameter along the direction of the applied stress. Furthermore, the inflection point in the $p^*(\sigma_3)$ curve identifies the transition stress which coincides with σ_3^{tr} for the structural transition. Therefore, we conclude that at $\sigma_3^{tr} = 0.23$ GPa, the material undergoes a first-order-like stress-induced ferroelectric structural phase transition from paraelectric cubic phase to ferroelectric tetragonal phase.

Below the transition stress σ_3^{tr} the dipoles are disordered and populate the states in the phase space almost uniformly. This ensemble is associated with large entropy and zero ferroelectric order parameter. Upon the stress induced transition the electric dipoles are forced to "order" by condensing near their preferred tetragonal state d_0 (or equivalently $-d_0$). From the microscopic point of view this transition greatly reduces the number of allowable states to be occupied by the dipoles, "squeezing" them into a smaller portion of configurational phase space. This reduces the "uncertainty" of the macroscopic state[26] giving rise to a large decrease in the isothermal entropy which is the signature of giant caloric effects. If adiabatic conditions are imposed dictating conservation of the total entropy, the stress-induced transition will produce a large change in temperature, which is another signature of giant caloric effects. This is consistent with our data in Fig. 1(a) where we observe a sharp increase of ΔT in post transition region.

We believe that the computational discovery of giant elastocaloric effect in ferroelectric alloys is an important step toward understanding the general phenomenon of giant caloric responses. It is particularly valuable in light of the fact that this effect coexists with another giant caloric effect in the same material, namely the electrocaloric effect. Such multicaloric nature of some ferroics could lead to new ways for achieving room temperature solid-state refrigeration.

*slisenk@usf.edu

[1] V. K. Pecharsky and K. A. Gschneidner, Jr., Phys. Rev. Lett. **78**, 4494 (1997).

[2] A. de Campos, D. L. Rocco, A. M. G. Carvalho, L. Caron, A. A. Coelho, S. Gama, L. M. da Silva, F. C. G. Gandra, A. O. dos Santos, L. P. Cardoso, P. J. von Ranke, and N. A. de Oliveira, Nat. Mater. **5**, 802 (2006).

[3] O. Tegus, E. Bruck, K. H. J. Buschow, and F. R. de Boer, Nature (London) **415**, 150 (2002).

[4] J. Liu, T. Gottschall, K. P. Skokov, J. D. Moore, and O. Gutfleisch, Nat. Mater. **11**, 620 (2012).

[5] L. Manosa, D. Gonzalez-Alonso, A. Planes, E. Bonnot, M. Barrio, J.-L. Tamarit, S. Aksoy, and M. Acet, Nat. Mater. **9**, 478 (2010).

[6] L. Manosa, D. Gonzalez-Alonso, A. Planes, M. Barrio, J.-L. Tamarit, I. S. Titov, M. Acet, A. Bhattacharyya, and S. Majumdar, Nature Commun. **2**, 595 (2011).

[7] E. Bonnot, R. Romero, L. Mañosa, E. Vives, and A. Planes, Phys. Rev. Lett. **100**, 125901 (2008).

[8] A. S. Mischenko, Q. Zhang, J. F. Scott, R. W. Whatmore, and N. D. Mathur, Science **311**, 1270 (2006).

[9] B. Neese, B. Chu, S.-G. Lu, Y. Wang, E. Furman, and Q. Zhang, Science **321**, 821 (2008).

[10] K. A. GschneidnerJr, V. K. Pecharsky, and A. O. Tsokol, Rep. Prog. Phys. **68**, 1479 (2005).

[11] J. F. Scott, Annu. Rev. Mater. Sci. **41**, 229 (2011).

[12] S.-G. Lu and Q. Zhang, Adv. Mater. **21**, 1983 (2009).

[13] S. Fahler, U. K. Robler, O. Kastner, J. Eckert, G. Eggeler, H. Emmerich, P. Entel, S. Muller, E. Quandt, and K. Albe, Advanced Engineering Materials **14**, 10 (2012).

[14] It is important to emphasize that any piezoelectric material exhibits the coupling between electric polarization and structural distortion.

[15] G. Akcay, S. P. Alpay, J. V. Mantese, and G. A. Rossetti, Jr., Appl. Phys. Lett. **90**, 252909 (2007).

[16] I. Ponomareva and S. Lisenkov, Phys. Rev. Lett. **108**, 167604 (2012).

[17] S. Lisenkov and I. Ponomareva, Phys. Rev. B **80**, 140102 (2009).

[18] V. V. Lemanov, E. P. Smirnova, P. P. Syrnikov, and E. A. Tarakanov, Phys. Rev. B **54**, 3151 (1996).

[19] L. Walizer, S. Lisenkov, and L. Bellaiche, Phys. Rev. B **73**, 144105 (2006).

[20] I. Ponomareva, L. Bellaiche, T. Ostapchuk, J. Hlinka, and J. Petzelt, Phys. Rev. B **77**, 012102 (2008).

[21] S. Lisenkov and L. Bellaiche, Phys. Rev. B **76**, 020102 (2007).

[22] S. Lisenkov, I. Ponomareva, and L. Bellaiche, Phys. Rev. B **79**, 024101 (2009).

[23] N. Choudhury, L. Walizer, S. Lisenkov, and L. Bellaiche, Nature (London) **470**, 513 (2011).

[24] M. Creutz, Phys. Rev. Lett. **50**, 1411 (1983).

[25] N. Metropolis, A. Rosenbluth, M. Rosenbluth, and A. Teller, J. Chem. Phys. **21**, 1087 (1953).

[26] E. A. Jackson, *Equilibrium Statistical Mechanics* (Prentice-Hall, Inc., Englewood Cliffs, New Jersey, 1968), Chap. 3.